

ORIGINAL RESEARCH

Effects of Imatinib Combined With Everolimus on Mouse Pituitary Tumor Cell AtT-20

Wenxin Wang, MSc; Yi Lin, MSc; Xinguo Qu, MSc; Linghu Meng, MSc; Jianquan Yang, MSc

ABSTRACT

Context • Pituitary adenoma is a clinical syndrome in which excessive production of pituitary corticotropin (ACTH). For ACTH tumor cells, researchers know little about the influence of the cell-cycle process on ACTH production and cell proliferation. Some research has shown that imatinib can induce apoptosis of tumor cells.

Objective • The study intended to explore the effects and molecular mechanisms of imatinib combined with everolimus on AtT-20 cells in AtT-20 mouse pituitary tumors.

Design • The research team performed a laboratory study using murine corticotropin tumor AtT-20 cells.

Setting • The study took place at the Department of Neurosurgery at Renmin Hospital of the Hubei University of Medicine in Shiyan, Hubei, China.

Intervention • The research team cultured the cells in AtT-20-cell-specific medium containing 100 µg/mL of streptomycin, 100 U/mL of penicillin, and 10% fetal bovine serum at 37°C and 5% CO₂. The team divided the cells into a control group, a normal culture without the drug, and an intervention group, incubated for 24 hours with 1 µM of imatinib and 3 µM of everolimus when the cells grew to 40% confluence.

Outcome Measures • The research team: (1) determined the effects of the combined drugs on cell viability using a methyl thiazolyl tetrazolium (MTT) assay; (2) detected the cell's mitochondrial membrane potential and LDH leakage using "sytox blue, 5',6,6'-tetrachloro-1,1',3,3'-tetraethylbenzimidazolylcarbocyanine iodide," CBIC2(3) or JC-1, and lactate dehydrogenase (LDH) assay kits, respectively; (3) detected AtT-20 cell apoptosis using a "terminal deoxynucleotidyl transferase (TdT)-mediated deoxyuridine triphosphate (dUTP) nick-end labeling" (TUNEL) kit; (4) analyzed the expression of protein kinase B (p-Akt), cAMP-response element binding protein (p-CREB), p27, p53, and cyclin E using a Western blot

test; (5) detected the mRNA expression of opioid melanin procorticotropin (POMC), caspase-3, and pituitary tumor transforming gene 1 (PTTG1) using reverse transcription-polymerase chain reaction (RT-PCR); (6) measure the concentration of adreno-cortico-tropic-hormone (ACTH) in the supernatant using an enzyme-linked immunoassay (ELISA) kit; and (7) assessed the cell cycle distribution using flow cytometry.

Results • No differences existed in cell viability between the groups at the baseline (0 h) of the culture period ($P > .05$). Compared to the control group, the intervention group's: (1) cell viability was significantly lower at 4, 8, and 12 hours and postintervention at 16 hours ($P < .001$); (2) LDH concentration was significantly higher ($P < .001$); (3) mitochondrial membrane potential was significantly lower ($P < .001$); (4) apoptosis rate of TUNEL was significantly higher ($P < .001$); (5) expression of p-Akt, p-CREB phosphorylation, and cyclin E was significantly lower ($P < .001$), (6) expression of p27 and p53 protein was significantly higher ($P < .001$); (7) mRNA expression of POMC and PTTG1 were significantly lower ($P < .001$); (8) mRNA expression of caspase-3 was significantly higher ($P < .001$); (9) concentration of ACTH was lower ($P < .001$); and (10) percentage of cells in the G0/G1 phase was significantly higher, while the percentage of cells in the S phase was significantly lower ($P < .05$).

Conclusions • Imatinib combined with everolimus can affect the AtT-20 cell cycle through the signaling pathway of the phosphatidylinositol-3-kinase (PI3K)/Akt/protein kinase A (PKA) system and can inhibit cell proliferation and induce cell apoptosis. Therefore, Imatinib and everolimus may be an effective combination of candidates for drugs for mouse pituitary tumor. (*Altern Ther Health Med.* 2023;29(1):238-244).

Wenxin Wang, MSc; Yi Lin, MSc; Xinguo Qu, MSc; Linghu Meng, MSc; Jianquan Yang, MSc; Department of Neurosurgery, Renmin Hospital, Hubei University of Medicine, Shiyan, Hubei, China.

Corresponding author: Jianquan Yang, MSc
E-mail: 1209691292@qq.com

Pituitary adenoma is a clinical syndrome in which excessive production of pituitary corticotropin (ACTH) causes hypercortisolemia.¹ This can lead to osteoporosis, infection, hyperglycemia, hypertension, and atherosclerosis.²⁻⁴ Surgical resection of the pituitary adenoma is the main treatment, but the curative operation is challenging.⁵

ACTH adenoma secretes adrenocorticotrophic hormone autonomously.⁶ Drugs for ACTH that target adenoma secretions include cabergoline and somatostatin analogues, but these still aren't common as standard treatments.

POMC

The precursor of ACTH, opioid melanin procorticotropin (POMC), is split into β -lipotropic hormone and ACTH by the processing enzyme prohormone convertase (PC)-1/3.⁷ Pivonello et al and de Vries et al found that the corticotropin releasing factor (CRF) in ACTH cells can induce transcription of opioid melanin procorticotropin (POMC) and ACTH secretion through the cAMP-protein kinase A (APKA) pathway.⁸ de Vries F et al found that CRF can increase phosphorylation of the cAMP-response element binding protein (CREB) through the PKA pathway in AtT-20 cells.⁹ The PKA pathway plays an important role in POMC gene regulation and CRF1 receptor desensitization in ACTH cells.¹⁰

In AtT-20, the protein kinase C (PKC) pathway is known to increase intracellular Ca^{2+} , thus promoting ACTH secretions.¹¹ In AtT-20 cells, the PKC pathway is also involved in POMC gene expression.¹² Therefore, the PKA and PKC pathways may participate in gene regulation through CREB phosphorylation in AtT-20 cells.

The production of ACTH may be coordinated with the cell proliferation of tumor cells.¹³ However, for ACTH tumor cells, researchers know little about the influence of the cell-cycle process on ACTH production and cell proliferation.

Apoptosis of Tumor Cells

Lactate dehydrogenase (LDH) is used as a marker of apoptosis in the cytosolic proteins, because its enzyme activity is easy to measure. LDH is a key glycolytic enzyme, which can oxidize lactic acid to pyruvic acid and transfer electrons to the cofactor nicotinamide adenine dinucleotide (NAD⁺) to form NADH [NAD + hydrogen (H)].¹⁴

The general characteristics of apoptosis include mitochondrial membrane depolarization, caspase-3 activation, and DNA fragmentation. The ACTH level depends on cell synthesis and cell proliferation. Therefore, a decrease in cell growth caused by apoptosis can lead to a decrease in the ACTH level observed in a culture medium.

Mitochondrial damage plays a central role in most cell-death processes, especially programmed cell-death pathways. Mitochondrial damage is characterized by a variety of biochemical events, including changes in energy production, permeability of the outer membranes of mitochondria, release of the pro-apoptotic BCL-2 (B-cell CLL/lymphoma 2) family proteins, and loss of the inner membrane potential of mitochondria.¹⁵

Osorio et al found that imatinib and phenytoin can induce apoptosis of tumor cells.¹⁶ Imatinib is a selective TK (transketolase) inhibitor, and it's currently the first-line treatment for chronic myeloid leukemia.¹⁷ Imatinib represents an example of a new class of anticancer agents.¹⁸ Phenytoin is an anticonvulsant for treatment and prevention of seizures

Imatinib is a well-designed, oral, signal transduction inhibitor that specifically targets several protein tyrosine kinases. Mohammadi and Gelderblom found that it can have remarkable anticancer activity in patients with chronic myeloid leukemia and malignant gastrointestinal stromal tumors.¹⁹ Kim et al found that imatinib and everolimus is a treatment for cancer of the kidney, pancreas, breast, and brain, can have antitumor effects on glioma cells, osteosarcoma cells, and gastric cancer cells.²⁰ However, a recent study found that imatinib can inhibit growth-hormone (GH) secretion in GH tumor cells without affecting cell activity.²¹

Att-20 is a mouse pituitary tumor cell, which can be used for in vitro study of pituitary tumor.²² Pituitary tumor transforming gene 1 (PTTG1), known as the separate suppressor protein gene, is an oncogene found in rat pituitary tumors in recent years. It can not only bind to the separate and inactivate the separate, thus inhibiting the separation of sister chromatids, but also has transcriptional activation activity.²³ Imatinib and everolimus can inhibit the proliferation of AtT-20 cells and induce DNA fragmentation in ACTH tumor cells, indicating that inhibitors can induce cell death in tumor cells. Pituitary tumor transforming gene 1 (PTTG1), an oncogene cloned from rat pituitary adenoma, can trigger the development of pituitary adenoma and can activate cell proliferation. A positive correlation exists between PTTG1 and histone deacetylase or heat shock protein 90.

Rapamycin

Rapamycin, a natural antifungal antibiotic, is a selective inhibitor of the mammalian target of rapamycin (mTOR), serine-threonine protein kinase, which is a potent inhibitor of the growth and proliferation of tumor cells, endothelial cells, fibroblasts, and vascular smooth muscle cells. It can inhibit the glycolysis of solid tumors in vitro and in vivo²⁴⁻²⁷ and is an immunosuppressant that binds to FK binding protein 12 (FKBP 12).²⁸ Everolimus is a mammalian target of rapamycin (mTOR) kinase inhibitor.

The phosphoinositide 3-kinase (PI3K)/Akt/mammalian target of the rapamycin pathway is an intracellular signal transduction pathway, which can contribute to apoptosis.^{29,30} This pathway can be overactive, thus reducing apoptosis and allowing proliferation in various cancer cells. In fact, compared with normal pituitary cells, the expression level of Akt in pituitary tumors, including ACTH tumor cells, is upregulated. Therefore, the Akt pathway may be involved in pituitary cell proliferation.

Senkus et al found that imatinib and phenytoin could increase the levels of p27 and p53 in cells while decreasing the level of cyclin E.²¹ P27 and p53 are tumor suppressor proteins that regulate cyclin-dependent proteins, thus inhibiting cell cycle.^{32,33}

The current study intended to explore the effects and molecular mechanisms of imatinib combined with everolimus on AtT-20 cells in AtT-20 mouse pituitary tumors.

METHODS

Procedures

The research team performed a laboratory study using murine corticotropin tumor AtT-20 cells. The study took place at the Department of Neurosurgery at Renmin Hospital of the Hubei University of Medicine in Shiyan, Hubei, China.

Cell culture and groups. The research team: (1) obtained murine corticotropin tumor AtT-20 cells—mouse pituitary tumor cells, from (American Type Culture Collection (ATCC), Rockefeller City, Maryland, USA); (2) cultured the cells in AtT-20-cell-specific medium (Wuhan Procel Corporation, Wuhan, Hubei, China) containing 100 µg/mL of streptomycin, 100 U/mL of penicillin and 10% fetal bovine serum at 37°C and 5% CO₂; (3) used Dulbecco's Modified Eagle Medium (DMEM) from Wuhan Yipu Biotechnology Co., Ltd (Wuhan, Hubei, China) supplemented with 0.2% bovine serum albumin, at night before each experiment; (4) divided the cells into the control group, which included cells from a normal culture with no drugs, and the intervention group, which included cells that were incubated with one µM of imatinib and 3 µM of everolimus for 24 hours after they grew to 40% confluence; (5) collected the total cell RNA or protein at the end of each experiment and stored it at -80°C until a relevant determination was made; (6) imatinib (Zhengzhou Aikem Chemical Co. LTD, Zhengzhou, Henan, China); and (6) everolimus (Wuhan Ding Xin Tong Pharmaceutical Co., LTD, Wuhan, Hubei, China).

Interventions

Cell viability analysis. The research team: (1) determined cell viability using an MTT assay (Shanghai Biyuntian Company, Shanghai, China); (2) inoculated the AtT-20 cells (5×10⁴ cells/ml) in a 96-well plate and incubated them overnight; (3) incubated the cells again after 4, 8, and 12 hours and postintervention at 16 hours of treatment with imatinib and everolimus, with one mg/ml of methyl thiazolyl tetrazolium (MTT) solution at 37°C for 4 hours; (4) added 100 µl of dimethyl sulfoxide (DMSO) from Shanghai Biyuntian Company (Shanghai, China) to dissolve the formazan crystals; and (5) examined cell viability expressed as a percentage of the control group using a 570 nm microplate reader (Amtran Electronics Technology (Shanghai) Co., LTD, Shanghai, China).

Lactate dehydrogenase (LDH) leakage and mitochondrial membrane potential detection. The research team: (1) inoculated the AtT-20 cells (5 × 10⁴ cells/ml) in a six-well plate and incubated them overnight; (2) detected LDH leakage after 16 hours of treatment with imatinib and everolimus, according to the manufacturer's instructions, using an LDH assay kit (Nanjing Jiancheng Bioengineering Research Institute, Nanjing, China;) (3) detected mitochondrial membrane potential using JC-1 dye (Shanghai Maokang Biotechnology Co., LTD, Shanghai, China); (4) cultured the AtT-20 cells (1×10⁵ cells /ml) in six-well plates; (5) incubated them with 2 mm of JC-1 at 37°C for 30 minutes; and (6) analyzed the cells using FACSCalibur (Franklin Lakes, New Jersey, US) flow cytometry.

Terminal deoxynucleotidyl transferase (TdT)-mediated deoxyuridine triphosphate (dUTP) nick end labeling (TUNEL). The research team: (1) detected DNA fragmentation of apoptotic AtT-20 cells using a TUNEL kit (Wuhan Antejie Biotechnology Co., LTD, Wuhan, China); (2) inoculated the AtT-20 cells (1 × 10⁵ cells /ml) in a six-well plate and treated them with imatinib and everolimus at prescribed concentrations for 12 hours; (3) incubated the cells with terminal deoxynucleotidyl transferase (TdT) at 37°C for one hour and with antidigoxin conjugate for 30 minutes; (4) stained the nucleus with "4',6-Diamidino-2-phenylindole dihydrochloride" (DAPI); and (5) captured the fluorescent image using a fluorescence microscope (Leica Microsystems, Wetzlar, Germany).

Western blot. The research team analyzed the expression level of protein using a Western blot. The team: (1) prepared total cytoplasm and nucleoprotein extracts using a cytosol kit and a nucleoprotein extraction kit, respectively (Thermo Fisher Scientific (China) Co., LTD, Shanghai, China); (2) determined the total protein concentration using a dioctanoic acid assay; (3) separated 20 µg of protein using 10% sodium dodecyl-sulfate polyacrylamide gel electrophoresis (SDS-PAGE) and transferred it to a polyvinylidene fluoride (PVDF) membrane; (4) blocked the membrane with 2% bovine serum albumin (BSA) from Sigma-Aldrich (St Louis, Missouri, USA) and 0.1% tris buffered saline (TBS)-Tween-20 solution (Shanghai Biyuntian Company, Shanghai, China) at 4°C for one hour; (5) incubated the membrane overnight with the following primary antibodies from Abcam (Cambridge, Massachusetts, USA), at 4°C: P-CREB (1:200); p-Akt (1:200); p27(1:200); p53(1:200); Cyclin E (1:200); and β-actin (1:1000); (6) incubated the membrane at 4°C for one hour with the corresponding horseradish peroxidase-coupled goat anti-mouse antibody (1:400, Abcam) or goat anti-rabbit secondary antibody (1:400, Abcam); (7) visualized an immunoblot using an enhanced chemical aequorin blot detection kit (Shanghai Biyuntian Company, Shanghai, China) and a molecular imager with Image Lab 3.0 (Bio-Rad, Hercules, California, USA); (8) determined the equivalent loading of protein by β -actin or laminin B; and (9) quantified the expression level of protein using a densitometer molecular device (Bio-Rad, Hercules, California, USA).

Quantitative, real-time, reverse transcription-polymerase chain reaction (RT-PCR). The research team: (1) evaluated the expression level of mRNA using quantitative real-time PCR and specific primers and probe sets; (2) amplified the sample using the following cycle parameters: 95°C for 10 minutes, 40 cycles of 95°C for 15 seconds, and 60°C for one minute; (3) collected and recorded the data using ABI PRISM 7000 SDS software (American Applied Biosystems Company, Newark, Delaware, US) and expressed it as a function of the threshold cycle (CT); (4) calculated the relative gene expression using the 2-ΔΔCT method; in short, determined the CT of the reaction between the amplification target gene and the reference gene for each analyzed sample; (5) corrected the CT of the gene

of interest of each sample by subtracting the CT (Δ CT) of the housekeeping gene; (6) selected the untreated control as the reference sample, with the Δ CT of all experimental samples decreasing the average Δ CT($\Delta\Delta$ CT) of the control sample; and (7) used the formula $2^{-\Delta\Delta$ CT to calculate the abundance of experimental mRNA relative to control mRNA.

Cell cycle analysis. The research team: (1) incubated the AtT-20 cells with 10μ of aphidicolin or a carrier (DMSO) for 24 hours; (2) collected the cells using trypsin digestion; (3) centrifuged and suspended them in Triton X-100 (MP Biomedicals, Santa Ana, California, US); (5) treated the cells with 0.5% RNase at 37°C for 30 minutes; (6) stained the cells with $50\ \mu\text{g}/\text{mL}$ propidium iodide; (7) analyzed the DNA content of cells using fluorescence activated cell sorting (FACS) from Thermo Fisher Scientific (China) Co., LTD (Shanghai, China); and (8) used BDFACSDiva software (Becton, Dickinson and Company, Franklin Lakes, New Jersey, US) to determine the cell-cycle map.

G0/G1 period and S Period. G0 phase: The period in which cells in a dividing tissue temporarily break out of the cell cycle and enter a state of cessation of cell division. G1 phase: DNA synthesis, RNA and ribosome synthesis. S phase: DNA replication phase, which is mainly the replication of genetic material, namely the synthesis of DNA, histones and enzymes needed for replication. The cell cycle was analyzed by flow cytometry.

Outcome Measures

AtT-20 cell viability. The research determined the influence of the combined drugs on cell viability. Treatment with imatinib and everolimus resulted in decreased viability of ATT-20 cells, mitochondrial membrane potential destruction, caspase-3 activation, DNA fragmentation, and decreased POMC mRNA expression and ACTH expression in the medium of the intervention group. These results indicated that imatinib and everolimus could induce apoptosis in ATT-20 cells.

Mitochondrial membrane potential and LDH leakage. The research team detected the cells' mitochondrial membrane potential and LDH leakage. After treatment with imatinib and everolimus, LDH release increased and mitochondrial membrane potential decreased in AT-20 cells, indicating the occurrence of apoptosis.

Apoptosis. The research team detected the apoptosis of the AtT-20 cells. The apoptosis of ATT-20 cells induced by imatinib combined with everolimus was significantly higher than that of control group.

p-Akt, p-CREB, and Cyclin E. The research team analyzed the expression of p-Akt, p-CREB phosphorylation, p27, p53 and cyclin E in cells. The expressions of p-Akt, p-CREB phosphorylation and cyclin E in the intervention group were lower than those in the control group, while the expressions of p27 and p53 in the intervention group were significantly higher than those in the control group.

POMC, caspase-3 and PTTG1. The research team detected the mRNA expressions of POMC, caspase-3 and

PTTG1 in cells. The mRNA expressions of POMC and PTTG1 in the intervention group were significantly lower than those in the control group. The expression of caspase-3 mRNA in the intervention group was significantly higher than that in the control group.

ACTH concentration. The research team measured the ACTH concentration in supernatant. The concentration of ACTH in the intervention group was significantly lower than that in the control group.

Cell cycle analysis. The research team evaluated the cell-cycle distribution. The percentage of cells in G0/ G1 phase in the intervention group was significantly higher than that in the control group, and the percentage of cells in S phase was significantly lower than that in the control group.

G0/G1 period and S Period. The percentage of cells in G0/ G1 phase in the intervention group was significantly higher than that in the control group, and the percentage of cells in S phase was significantly lower than that in the control group.

Statistical Analysis

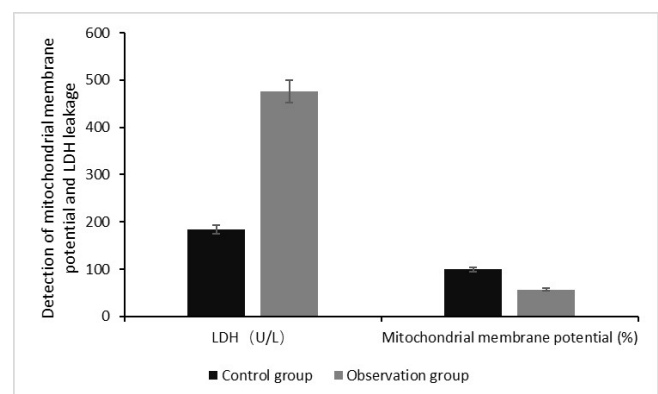
The data represented the results from three independent experiments. The research team expressed the results as the standard errors of the mean values. The team used Student's two-tailed *t* test for comparisons between the two groups and one-way analysis of variance (ANOVA) and Bonferroni's multiple comparison tests for comparisons between multiple groups. $P < .05$ was considered to be statistically significant.

RESULTS

AtT-20 Cell Viability

Figure 1 and Table 1 show that no difference existed between the groups in the cell viability of the cultures at baseline at zero hours ($P > .05$), but the intervention group's cell viability was significantly lower than that of the control group at 4 h, 8 h, and 12 h, and postintervention at 16 h, with $P < .001$ for all time points. Imatinib combined with everolimus can significantly inhibit the cell viability of the AtT-20 cells.

Figure 1. Cell Viability as Determined by MTT Assay



Abbreviations: MTT, methyl thiazolyl tetrazolium.

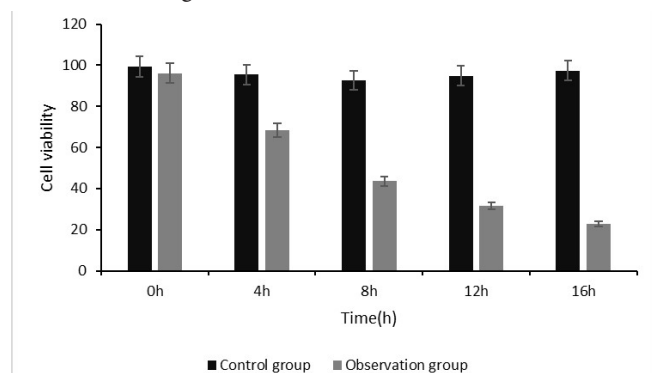
Table 1. Cell Viability as Determined Using MTT Assay (n = 30)

Groups	Baseline (0 h) Mean ± SD	4h Mean ± SD	8h Mean ± SD	12h Mean ± SD	Postintervention (16h) Mean ± SD
Control group	99.32 ± 15.83	95.51 ± 8.46	92.62 ± 7.30	94.82 ± 5.24	97.38 ± 15.19
Intervention group	96.19 ± 17.26	68.36 ± 11.47	43.55 ± 9.11	31.57 ± 7.25	22.77 ± 4.28
<i>t</i> value	0.732	10.434	24.899	38.728	25.895
<i>P</i> value	.467	<.001 ^a	<.001 ^a	<.001 ^a	<.001 ^a

^a*P* < .001, indicating that the intervention group's cell viability was significantly lower than the control group's at 4, 8, and 12 hours and postintervention at 16 hours

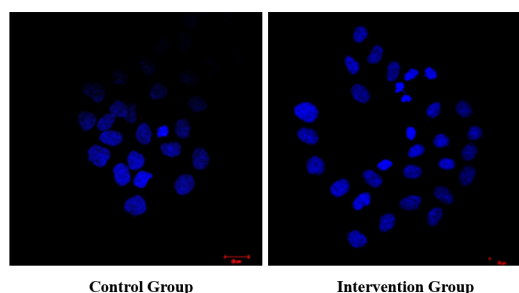
Abbreviations: MTT, methyl thiazolyl tetrazolium.

Figure 2. Detection of Mitochondrial Membrane Potential and LDH Leakage



Abbreviations: LDH, lactate dehydrogenase.

Figure 3. Apoptosis Detected Using TUNEL



Abbreviations: TUNEL, terminal deoxynucleotidyl transferase (TdT)-mediated deoxyuridine triphosphate (dUTP) nick-end labeling.

Mitochondrial Membrane Potential and LDH Leakage

Figure 2 and Table 2 show that the intervention group's LDH concentration was significantly higher and the mitochondrial membrane potential was significantly lower than those of the control group postintervention, with *P* < .001 for both. Imatinib combined with everolimus can destroy the cell membrane and mitochondrial structure of AtT-20 cells.

Apoptosis

The intervention group's TUNEL apoptosis rate was significantly higher than that of the control group

Table 2. Detection of Mitochondrial Membrane Potential and LDH Leakage Postintervention (n = 30)

Groups	LDH U/L Mean ± SD	Mitochondrial Membrane Potential (%) Mean ± SD
Control group	183.25 ± 33.59	99.35 ± 3.27
Intervention group	475.88 ± 62.68	56.18 ± 7.44
<i>t</i> value	-22.385	29.095
<i>P</i> value	<.001 ^a	<.001 ^a

^a*P* < .001, indicating that the intervention group's LDH was significantly higher and mitochondrial membrane potential was significantly lower than the control group's postintervention

Abbreviations: LDH, lactate dehydrogenase.

Table 3. Apoptosis Detected Postintervention (n = 30) Using TUNEL

Groups	TUNEL Apoptosis Mean ± SD
Control group	14.68 ± 3.22
Intervention group	58.49 ± 16.25
<i>t</i> value	-14.485
<i>P</i> value	<.001 ^a

^a*P* < .001, indicating that the intervention group's apoptosis rate was significantly higher than the control group's postintervention

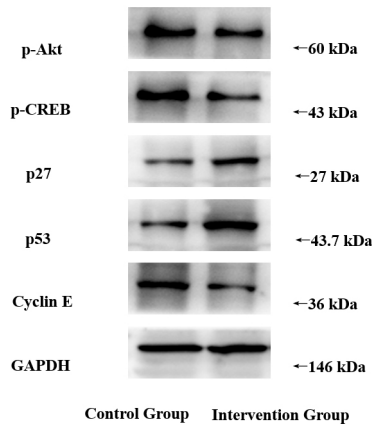
Abbreviations: TUNEL, terminal deoxynucleotidyl transferase (TdT)-mediated deoxyuridine triphosphate (dUTP) nick-end labeling.

postintervention (*P* < .001). Table 3 shows that the TUNEL apoptosis rate of the control group was 14.68 ± 3.22 and of the intervention group was 58.49 ± 16.25. The DNA fragmentation of the intervention group's apoptotic AtT-20 cells was significantly higher than that of the control group (Figure 3).

p-Akt, p-CREB, and Cyclin E

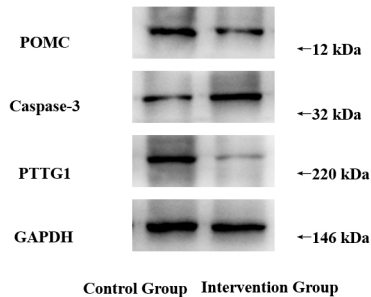
Figure 4 and Table 4 show that the intervention group's expression of p-Akt, p-CREB phosphorylation, and cyclin E was significantly lower postintervention than that of the control group (*P* < .001), while the intervention group's

Figure 4. Expression Levels of P-Akt, p-CREB, p27, p53 and Cyclin E Using Western Blot Analysis



Abbreviations: GAPDH, glyceraldehyde-3-phosphate dehydrogenase; p-Akt, protein kinase B; p-CREB, cAMP-response element binding protein.

Figure 5. Detection of mRNA Expression of POMC, Caspase-3, and PTTG1 in Cells Using RT-PCR



Abbreviations: GAPDH, glyceraldehyde-3-phosphate dehydrogenase; POMC, pro-opiomelanocortin; PTTG1, pituitary tumor transforming gene 1.

expression of p27 and p53 protein was significantly higher than that of the control group ($P < .001$).

POMC, Caspase-3, and PTTG1

Figure 5 and Table 5 show that the intervention group's mRNA expressions of POMC and PTTG1 were significantly lower postintervention than those of the control group ($P < .001$). The intervention group's mRNA expressions of caspase-3 was significantly higher than that of the control group postintervention ($P < .001$).

Table 4. Expression Levels of P-Akt, p-CREB, p27, p53 and Cyclin E Postintervention Using Western Blot Analysis (n = 30)

Groups	p-Akt Mean ± SD	p-CREB Mean ± SD	p27 Mean ± SD	p53 Mean ± SD	Cyclin E Mean ± SD
Control group	1.95 ± 0.16	1.97 ± 0.14	1.05 ± 0.08	1.04 ± 0.03	1.96 ± 0.35
Intervention group	1.02 ± 0.09	1.12 ± 0.08	1.87 ± 0.32	1.93 ± 0.47	1.05 ± 0.06
t value	27.748	28.873	-13.616	-10.351	14.036
P value	<.001 ^a				

^a $P < .001$, indicating that the intervention group's p-Akt, p-CREB, and Cyclin E were significantly lower and p27 and p53 were significantly higher than the control group's postintervention

Abbreviations: p-Akt, protein kinase B; p-CREB, p-cAMP-response element binding protein.

Table 5. Expression Levels of POMC, Caspase-3, and PTTG1 in Cells Postintervention Using RT-PCR (n = 30)

Groups	POMC Mean ± SD	Caspase-3 Mean ± SD	PTTG1 Mean ± SD
Control group	1.96 ± 0.16	1.02 ± 0.05	1.87 ± 0.13
Intervention group	1.05 ± 0.08	1.86 ± 0.27	1.14 ± 0.11
t value	27.863	16.755	23.479
P value	<.001 ^a	<.001 ^a	<.001 ^a

^a $P < .001$, indicating that the intervention group's POMC and PTTG1 were significantly lower and Caspase-3 was significantly higher than the control group's postintervention

Abbreviations: POMC, pro-opiomelanocortin; PTTG1, pituitary tumor transforming gene 1; RT-PCR, reverse transcription-polymerase chain reaction.

Table 6. Detection of ACTH Concentration Postintervention (n = 30)

Groups	ACTH pg/ml Mean ± SD
Control group	5637.25 ± 269.11
Intervention group	2325.49 ± 192.49
t value	54.824
P value	<.001 ^a

^a $P < .001$, indicating that the intervention group's ACTH was significantly lower than the control group's postintervention

Abbreviations: ACTH, adreno-cortico-tropic-hormone.

Table 7. Cell Cycle Analysis (n = 30)

Groups	G0/G1 Period Mean ± SD	S Period Mean ± SD
Control group	63.25 ± 7.44	38.55 ± 8.29
Intervention group	84.19 ± 19.28	16.37 ± 3.57
t value	5.550	13.459
P value	<.001 ^a	<.001 ^a

^a $P < .001$, indicating that the intervention group's percentage of G0/G1-phase cells was significantly higher and the percentage of S phase cells was significantly lower than the control group's postintervention

ACTH Concentration

Table 6 shows that the intervention group's ACTH concentration was significantly lower postintervention than that of the control group ($P < .001$).

Cell cycle analysis

Table 7 shows that the intervention group's percentage of G0/G1-phase cells was significantly higher than that of the control group, while the group's percentage of S phase cells was significantly lower than that in the control group ($P < .05$).

DISCUSSION

In the current study, treatment with imatinib and everolimus led to decreased cell viability, the destruction of mitochondrial membrane potential, caspases-3 activation, DNA fragmentation in AtT-20 cells, and decreased POMC mRNA expression and ACTH in the intervention group's culture medium. These results indicate that imatinib and everolimus can induce apoptosis of AtT-20 cells.

The current study's results also showed that the LDH release in AtT-20 cells increased and the mitochondrial membrane potential decreased after use of imatinib and everolimus, which both indicate the occurrence of apoptosis. The TUNEL kit showed that imatinib combined with everolimus could induce greater AtT-20 cell apoptosis as compared with the control group's apoptosis. In addition, the current study found that imatinib and everolimus reduced the expression of POMC mRNA in ACTH-secreting tumor cells and ACTH levels in the intervention group's culture medium.

The current study also found that imatinib and everolimus could reduce CREB phosphorylation and also could reduce Akt phosphorylation.

Researchers know that imatinib and everolimus can block cells upon entrance to the S phase, thus blocking the cell cycle. Flow cytometry analysis showed that imatinib and everolimus could reduce the percentage of S-phase cells and increase the percentage of G0/G1-phase cells in AtT-20 cells. The data indicated that imatinib and everolimus might induce G0/G1 cells to stay and inhibit the proliferation of AtT-20 cells.

CONCLUSIONS

The current research showed that imatinib combined with everolimus can affect the AtT-20 cell cycle through the signaling pathway of the phosphatidylinositol-3-kinase (PI3K)/Akt/protein kinase A (PKA) system and can inhibit cell proliferation and induce cell apoptosis. Therefore, imatinib and everolimus may be an effective combination of candidates for drugs for mouse pituitary tumor.

The limitation of this study is that no genetic intervention was performed to interpret the signaling pathways involved in this study, which will be conducted in the near future.

AUTHOR CONTRIBUTIONS

Wenxin Wang and Yi Lin contributed equally to this paper and should be regarded as co-first authors.

AUTHORS' DISCLOSURE STATEMENT

There are no potential conflicts of interest in this study.

REFERENCES

1. Wong C, Tang LH, Davidson C, et al. Two well-differentiated pancreatic neuroendocrine tumor mouse models. *Cell Death Differ*. 2020;27(11):269-283. doi:10.1038/s41418-019-0355-0
2. Barry S, Carlsen E, Marques P, et al. Tumor microenvironment defines the invasive phenotype of ALP-mutation-positive pituitary tumors. *Oncogene*. 2019;38(27):5381-5395. doi:10.1038/s41388-019-0779-5
3. Fagin JA, Petrini JH. Oncogene-induced DNA damage: cyclic AMP steps into the ring. *J Clin Invest*. 2020;130(11):5668-5670. doi:10.1172/JCI142237
4. Matsuno K, Nagashima S, Shiiba I, et al. MITOL dysfunction causes dwarfism with anterior pituitary hypoplasia. *J Biochem*. 2020;168(3):305-312. doi:10.1093/jb/mvaa050
5. Yang Z, Shi J, Xie J, et al. Large-scale generation of functional mRNA-encapsulating exosomes via cellular nanoporation. *Nat Biomed Eng*. 2020;4(1):69-83. doi:10.1038/s41551-019-0485-1
6. Almistehi WM, Vaninetti N, Mustafa S, et al. Secondary pituitary hormonal dysfunction patterns: tumor size and subtype matter. *Pituitary*. 2020;23(6):622-629. doi:10.1007/s11102-020-01067-7
7. Prodram F, Caputo M, Mele C, Marzullo P, Aimaretti G. Insights into non-classic and emerging causes of hypopituitarism. *Nat Rev Endocrinol*. 2021;17(2):114-129. doi:10.1038/s41574-020-00437-2
8. Pivonello R, Fleseriu M, Newell-Price J, et al; LINC 3 investigators. Efficacy and safety of osilodrostat in patients with Cushing's disease (LINC 3): a multicentre phase III study with a double-blind, randomised withdrawal phase. *Lancet Diabetes Endocrinol*. 2020;8(9):748-761. doi:10.1016/S2213-8587(20)30240-0
9. de Vries F, Lobatto DJ, Bakker LEH, van Furth WR, Biermasz NR, Pereira AM. Early postoperative HPA-axis testing after pituitary tumor surgery: reliability and safety of basal cortisol and CRH test. *Endocrine*. 2020;67(1):161-171. doi:10.1007/s12020-019-02094-6
10. Van Kolen K, Dautzenberg FM, Verstraeten K, et al. Corticotropin releasing factor-induced ERK phosphorylation in AtT20 cells occurs via a cAMP-dependent mechanism requiring EPAC2. *Neuropharmacology*. 2010;58(1):135-144. doi:10.1016/j.neuropharm.2009.06.022
11. MacEwan DJ, Johnson MS, Mitchell R. Protein kinase C isoforms in pituitary cells displaying differential sensitivity to phorbol ester. *Mol Cell Biochem*. 1999;202(1-2):85-90. doi:10.1023/A:1007090718274
12. McCerran BW, MacEwan DJ, Guild SB. Involvement of multiple protein kinase C isoforms in the ACTH secretory pathway of AtT-20 cells. *Br J Pharmacol*. 1995;115(2):307-315. doi:10.1111/j.1476-5381.1995.tb15878.x
13. van Lersel L, Li Z, Srivastava DK, et al. Hypothalamic-pituitary disorders in childhood cancer survivors: Prevalence, risk factors and long-term health outcomes. *J Clin Endocrinol Metab*. 2019;104(12):6101-6115. doi:10.1210/clinem.2019-00834
14. Yamaguchi H, Kamegawa A, Nakata K, et al. Leucine Dehydrogenase: structure and Thermostability. *Subcell Biochem*. 2021;96:355-372. doi:10.1007/978-3-030-58971-4_10
15. Cao X, Fu M, Bi R, et al. Cadmium induced BEAS-2B cells apoptosis and mitochondria damage via MAPK signaling pathway. *Chemosphere*. 2021;263:128346. doi:10.1016/j.chemosphere.2020.128346
16. Osorio S, Escudero-Vilaplana V, Gómez-Centurió I, González-Arias E, García-González X, Díez JL. Inadequate response to imatinib treatment in chronic myeloid leukemia due to a drug interaction with phenytoin. *J Oncol Pharm Pract*. 2019;25(3):694-698. doi:10.1177/1078155217743565
17. Cardoso HJ, Vaz CV, Carvalho TMA, Figueira MI, Socorro S. Tyrosine kinase inhibitor imatinib modulates the viability and apoptosis of castrate-resistant prostate cancer cells dependently on the glycolytic environment. *Life Sci*. 2019;218(12):274-283. doi:10.1016/j.lfs.2018.12.055
18. Jose A, Ninave KM, Karnam S, Venuganti VVK. Temperature-sensitive liposomes for co-delivery of tamoxifen and imatinib for synergistic breast cancer treatment. *J Liposome Res*. 2019;29(2):153-162. doi:10.1080/08982104.2018.1502315
19. Mohammadi M, Gelderblom H. Systemic therapy of advanced/metastatic gastrointestinal stromal tumors: an update on progress beyond imatinib, sunitinib, and regorafenib. *Expert Opin Investig Drugs*. 2021;30(2):143-152. doi:10.1080/13543784.2021.1857363
20. Kim JL, Lee DH, Jeong S, et al. Imatinib-induced apoptosis of gastric cancer cells is mediated by endoplasmic reticulum stress. *Oncol Rep*. 2019;41(3):1616-1626.
21. Gupta P, Rai A, Mukherjee KK, et al. Imatinib Inhibits GH Secretion From Somatotropinomas. *Front Endocrinol (Lausanne)*. 2019;9:453. doi:10.3389/fendo.2018.00453
22. Nasri A, Unniappan S. Nucleobindin-derived nesfatin-1 and nesfatin-1-like peptide stimulate pro-opiomelanocortin synthesis in murine AtT-20 corticotrophs through the cAMP/PKA/CREB signaling pathway. *Mol Cell Endocrinol*. 2021;536:111401. doi:10.1016/j.mce.2021.111401
23. Tian X, Xu WH, Xu FJ, et al. Identification of prognostic biomarkers in papillary renal cell carcinoma and PTTG1 may serve as a biomarker for predicting immunotherapy response. *Ann Med*. 2022;54(1):211-226. doi:10.1080/07853890.2021.2011956
24. Ediriweera MK, Tennekoon KH, Samarakoon SR. Role of the PI3K/AKT/mTOR signaling pathway in ovarian cancer: biological and therapeutic significance. *Semin Cancer Biol*. 2019;59(10):147-160. doi:10.1016/j.semcancer.2019.05.012
25. Alzahrani AS. PI3K/Akt/mTOR inhibitors in cancer: at the bench and bedside. *Semin Cancer Biol*. 2019;59(10):92-111. doi:10.1016/j.semcancer.2019.07.003
26. Murugan AK. mTOR: role in cancer, metastasis and drug resistance. *Semin Cancer Biol*. 2019;59(10):92-111. doi:10.1016/j.semcancer.2019.07.003
27. Arenas DJ, Floess K, Kobrin D, et al. Increased mTOR activation in idiopathic multicentric Castleman disease. *Blood*. 2020;135(19):1673-1684. doi:10.1182/blood.2019002792
28. Jhanwar-Uniyal M, Wainwright JV, Mohan AL, et al. Diverse signaling mechanisms of mTOR complexes: mTORC1 and mTORC2 in forming a formidable relationship. *Adv Biol Regul*. 2019;72(5):51-62. doi:10.1016/j.jbior.2019.03.003
29. Rohrbacher L, Brauchle B, Ogrinc Wagner A, von Bergwelt-Baildon M, Bücklein VL, Subklewe M. The PI3K-selective inhibitor idelalisib induces T- and NK-cell dysfunction independently of B-cell malignancy-associated immunosuppression. *Front Immunol*. 2021;12(5):608625. doi:10.3389/fimmu.2021.608625
30. Zhong F, Liu S, Hu D, Chen L. LncRNA AC099850.3 promotes hepatocellular carcinoma proliferation and invasion through PRR11/PI3K/AKT axis and is associated with patients prognosis. *J Cancer*. 2022;13(3):1048-1060. doi:10.7150/jca.66092
31. Senkus E, Szade J, Pieczyńska B, Kunc M, Pliszka A, Jassen J. Are synchronous and metachronous bilateral breast cancers different? An immunohistochemical analysis focused on cell cycle regulation. *Histol Histopathol*. 2018;33(1):55-64.
32. Maros ME, Balla P, Micsik T, et al. Cell cycle regulatory protein expression in multinucleated giant cells of giant cell tumor of bone: do they proliferate. *Pathol Oncol Res*. 2021;27(5):643146. doi:10.3389/pore.2021.643146
33. Tsai YC, Kuo PL, Kuo MC, et al. The interaction of miR-3781-Skp2 regulates cell senescence in diabetic nephropathy. *J Clin Med*. 2018;7(12):468. doi:10.3390/jcm7120468